JOM, Vol. 75, No. 2, 2023
https://doi.org/10.1007/s11837-022-05557-w

Extraction of Valuable Components from Ti-Bearing Blast Furnace Slag Using Sulfuric Acid Calcination Process

SIQI HE[1,3] and YAN WANG[2]

1.—College of Resources and Environmental Engineering, Mianyang Normal University, Mianyang 621010, Sichuan, China. 2.—College of Environment and Resources, Southwest University of Science and Technology, Mianyang 621010, Sichuan, China. 3.—e-mail: hemiaohesiqi@163.com

This article presents a clean and efficient method for extracting Ti, Al, and Mg components from Ti-bearing blast furnace slag with sulfuric acid. TBFS was calcined with concentrated sulfuric acid and then leached with deionized water. Variables such as acid-slag ratio, calcination temperature, and calcination time were studied. It was shown that when TBFS was reacted with concentrated sulfuric acid with an acid to slag weight ratio of 1.4 at 130°C for 40 min, the percentage of Ti, Al, and Mg recovered from deionized water leaching was up to 82.85%, 93.16%, and 96.96%, respectively. A possible calcination mechanism is discussed, in which less SO_2 was generated than could be completely absorbed by water, and no $CaSO_4{\cdot}2H_2O$ formed during the reaction. The main phases found in the calcined slag were II-anhydrite, aluminum sulfate, titanium sulfate, and magnesium sulfate. This method solved an issue present in traditional H_2SO_4 leaching processes, in which substantial $CaSO_4{\cdot}2H_2O$ colloid would be produced and coat the TBFS particles, thus hindering the extraction of components.

INTRODUCTION

Ti-bearing blast furnace slag (TBFS) is a solid waste produced from the coarse smelting of pig iron from vanadium–titanium magnetite ore using the blast furnace process. Currently, over 70 million tons of TBFS exist in the Panzhihua-Xichang area of China. TBFS is associated with severe environmental problems such as groundwater contamination via the leaching of hazardous heavy metals and the emission of particulates into the surrounding air,[1] necessitating that it be disposed of properly. TBFS also contains a variety of metal components, making it a valuable resource. Among its main components are MgO and Ti_XO_Y, alkaline oxides, and Al_2O_3, an amphoteric oxide, all of which easily react with acid. Therefore, sulfuric acid leaching is the most frequently used method for processing TBFS components.

In the sulfuric acid leaching process, Ti, Al, and Mg components in TBFS are dissolved in sulfuric acid solution. Then, titanium dioxide (TiO_2), aluminum hydroxide ($Al(OH)_3$), magnesium hydroxide ($Mg(OH)_2$), and hydrotalcite are produced from the solution via thermal hydrolysis, stepwise precipitation, and the hydrothermal method.[2–6] This method is simple in operation and can extract many valuable components at the same time, making it a good research prospect. The mass fraction of sulfuric acid in the leaching method is generally $< 90\%$.[2,7,8] To achieve a better extraction effect, the practical dosage of the sulfuric acid is generally far greater than the theoretical demand dosage, and the reaction temperature is close to the liquid boiling point, resulting in the generation of a large amount of acid gas and discharge of a large amount of waste acid, which poses an environmental hazard. In addition, Ca^{2+} ions in TBFS easily react with sulfuric acid to form gypsum ($CaSO_4{\cdot}2H_2O$) colloids and adhere to the surface of TBFS particles, which inhibit the reaction and prevent the maximal extraction of components.[9]

To avoid the above issues, in the present study, TBFS is reacted with concentrated sulfuric acid at a temperature > 100°C and below its boiling point to convert the titanium, magnesium, aluminum, and calcium components into titanium sulfate, magnesium sulfate, aluminum sulfate, and anhydrous

(Received July 18, 2022; accepted September 29, 2022; published online October 20, 2022)

calcium sulfate. Following this, the soluble sulfate $Ti(SO_4)_2$, $MgSO_4$, and $Al_2(SO_4)_3$ in the calcinated slag are leached into the solution with deionized water. First, the process realizes the activation of components at temperatures below the boiling point of concentrated sulfuric acid, avoiding the production of acid gas. Second, it uses concentrated sulfuric acid as a calcination additive to avoid the addition of H_2O molecules, thus avoiding the formation of gypsum colloid, making the reaction more efficient, and improving the extraction rate of components.

EXPERIMENTAL SETUP

Mineralogical Analysis of TBFS

The TBFS samples cooled by water were collected from Panzhihua Iron and Steel Co., Ltd. (Sichuan, China). TBFS was dried at 106°C for 24 h and ground to a particle size of < 0.074 mm. The chemical composition of TBFS was analyzed by XRF (Panaco, Axios x-ray fluorescence spectroscopy), the mineral phase of TBFS was analyzed by XRD (Rigaku, Ultima IV x-ray diffractometer equipped with a Cn Kα radiation source), and the valences of Ti and Fe in TBFS were analyzed by XPS (KRATOS, XSAM800 x-ray photoelectron spectroscopy).

Experimental Procedure

The experimental procedure of extracting valuable components from TBFS using the sulfuric acid calcination process is shown in Figure S1 of online supplementary material; 10 g of TBFS was placed in a 100-ml ceramic crucible with a lid, and concentrated sulfuric acid was weighed and mixed with TBFS according to specific acid-slag ratio (1.0, 1.2, 1.4, 1.6). The mixture was stirred well with a glass rod and calcined in a tube programmed heating furnace at five different temperature conditions (100°C, 110°C, 120°C, 130°C, and 140°C) for a set length of time (20 min, 40 min, 60 min, 80 min). During the experiment, a wet pH test paper was placed at the air outlet of the tube furnace to detect the generation of acid gas. After calcination, 10 g of calcined slag was mixed with 60 mL of deionized water and leached for 60 min at 60°C. The components of Ti, Al, and Mg were transferred from the calcined slag to the leached solution, and solid–liquid separation was carried out by centrifugation. The contents of Ti, Al, and Mg in the leached solution were determined by titration, and the percentages of components extracted (R) were calculated according to Eq. 1:

$$R = \frac{m_2}{m_1} \times 100\% \quad (1)$$

where m_1 and m_2 are the masses of the components (Ti, Al, and Mg) in the TBFS and leached solution, respectively.

RESULTS AND DISCUSSION

Initial Characterization of TBFS

Figure 1 shows the XRD pattern of TBFS. Compared with the standard card, the diffraction peaks at $d_{121} = 2.706$ Å, $d_{202} = 1.914$ Å, $d_{123} = 1.557$ Å, and $d_{242} = 1.353$ Å belong to the characteristic diffraction peaks of perovskite (JCPDS42-0423). In addition, the pattern shows some amorphous structure: the chemical bond in this structure is easier to break and synthesize, which leads to the high chemical activity of TBFS.[10] Table I shows the XRF analysis results of TBFS. Its main chemical components are CaO, SiO_2, TiO_2, Al_2O_3, and MgO. It contains certain amounts of SO_3, Fe_2O_3, K_2O, MnO, Na_2O, and small amounts of F, BaO, SrO, and ZrO_2. Ti is a valence-variable element. Its valence states are analyzed by x-ray photoelectron spectroscopy, and the results are shown in Fig. 2. In the Ti2p spectrum, the peak with a binding energy of 458.4 eV can be divided into two peaks of 458.3 eV and 459.1 eV, corresponding to Ti2p3/2 of Ti_2O_3 and TiO_2, respectively. In addition, the peak with a binding energy of 464.4 eV can be divided into two peaks of 464 eV and 464.9 eV, corresponding to Ti2p1/2 of Ti_2O_3 and TiO_2, respectively.[11] This shows that there are two valence states of Ti (Ti^{4+}, Ti^{3+}) present. The main chemical reactions of TBFS and concentrated sulfuric acid are shown in Eqs. 1, 2, 3, and 4 as follows:

$$TiO_2 + H_2SO_4 = TiOSO_4 + H_2O \quad (2)$$

$$Ti_2O_3 + 3H_2SO_4 = 2TiOSO_4 + 3H_2O + SO_2 \quad (3)$$

$$MgO + H_2SO_4 = MgSO_4 + H_2O \quad (4)$$

$$Al_2O_3 + 3H_2SO_4 = Al_2(SO_4)_3 + 3H_2O \quad (5)$$

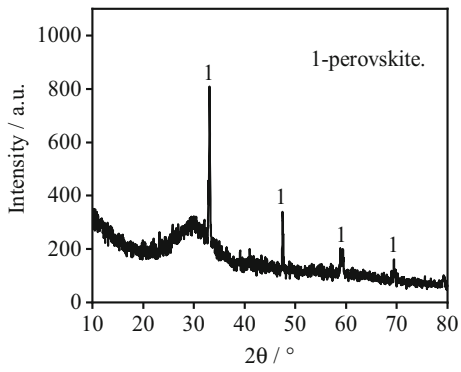

Fig. 1. XRD patterns of TBFS.

Table I. Chemical composition of TBFS

Compound	wt.%	Compound	wt.%
CaO	28.08	K_2O	0.72
SiO_2	26.74	MnO	0.64
TiO_2	19.65	Na_2O	0.53
Al_2O_3	13.86	F	0.17
MgO	7.64	BaO	0.07
SO_3	1.05	SrO	0.04
Fe_2O_3	0.79	ZrO_2	0.02

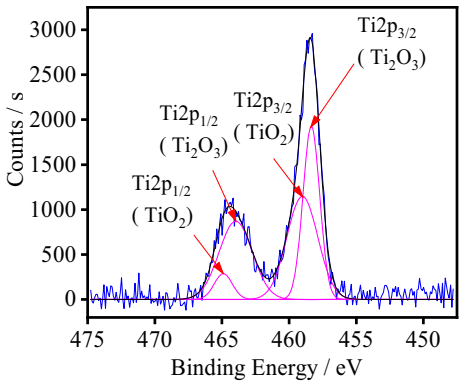

Fig. 2. XPS spectra of Ti2p regions in TBFS.

Effect of Acid-Slag Ratio on the Extraction of Ti, Mg, and Al from TBFS

Figure 3 shows the influence of the mass ratio of sulfuric acid to TBFS on the extraction rate of Ti, Mg, and Al components. During the experiment, the calcination temperature was 120°C and the calcination time was 60 min. When the amount of concentrated sulfuric acid is the theoretical consumption of Ti, Mg, Al and Fe components in TBFS reacting with it, the acid-slag ratio is set to 1:1, and the amount of sulfuric acid in the experiment is increased in equal proportion on this basis. As the acid-slag ratio increases, the extraction rates of Ti, Mg, and Al components increase first and then stabilize. When the acid-slag ratio was 1.4, the optimal extraction rates of Al, Mg, and Ti components were 95.19%, 95.34%, and 86.53%, respectively. Therefore, 1.4 was selected as the optimized acid-slag ratio. XRD analysis was carried out on the calcined slag obtained at different acid-slag ratios, the results of which are shown in Fig. 4a. The main phases found in the calcined slag were II-anhydrite (II-$CaSO_4$), aluminum sulfate ($Al_2(SO_4)_3$), titanium sulfate ($TiSO_4$), magnesium sulfate ($MgSO_4$), and some amorphous phases. The characteristic diffraction peak intensity of each phase is very weak, indicating that its crystallinity is poor. As the acid-slag ratio increases, the amorphous phase peak becomes noticeably wider and higher, and the number and intensity of characteristic diffraction peaks of aluminum sulfate, titanium sulfate, and

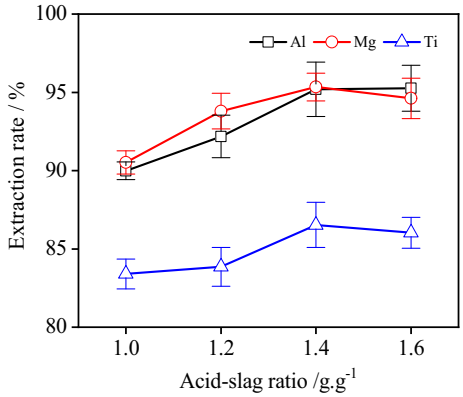

Fig. 3. Effect of acid-slag ratio on extraction rate of Ti, Mg, and Al components.

magnesium sulfate increase slightly, while the number and intensity of characteristic diffraction peaks of II-anhydrite decrease and then disappear. This occurs because the main factors influencing crystallization are temperature and time rather than acid-slag ratio: the increase of acid-slag ratio accelerates the reaction between the components and the sulfuric acid, but only results in the amount of these products increasing, while most of the products exist in amorphous form. The XRD pattern of water leached slag is shown in Fig. 4b. The main phase is shown to be gypsum ($CaSO_4{\cdot}2H_2O$), indicating the dissolution of II-anhydrite and its recrystallization into gypsum during the water leaching process. With the increased acid-slag ratio, the characteristic diffraction peak intensity of gypsum increases first and then decreases. This occurs because when the acid-slag ratio is < 1.2, the amount of II-anhydrite increases with the increasing acid-slag ratio during the calcination process, so the amount of gypsum recrystallized increases accordingly after water leaching, and the intensity of its characteristic diffraction peak increases. However, when the acid-slag ratio is > 1.2, there is more unreacted sulfuric acid involved in the calcination and leaching process, and the residual sulfuric acid may hinder the crystallization of gypsum, resulting in the decrease of the characteristic diffraction peak intensity.[12,13]

Effect of Calcination Temperature on the Extraction of Ti, Mg, and Al from TBFS

Figure 5 shows the effect of calcination temperature on the extraction rate of the components. During the calcination process, the acid-slag ratio was 1.4 and the reaction time 60 min. The results show that calcination temperature has a great influence on the extraction of Ti, Mg, and Al components. The extraction rate of each component increases first and then decreases with the increase of calcination temperature. Optimal extraction rates of 86.81% of Ti, 97.37% of Mg, and 96.03% of Al were obtained at a temperature of 130°C. The

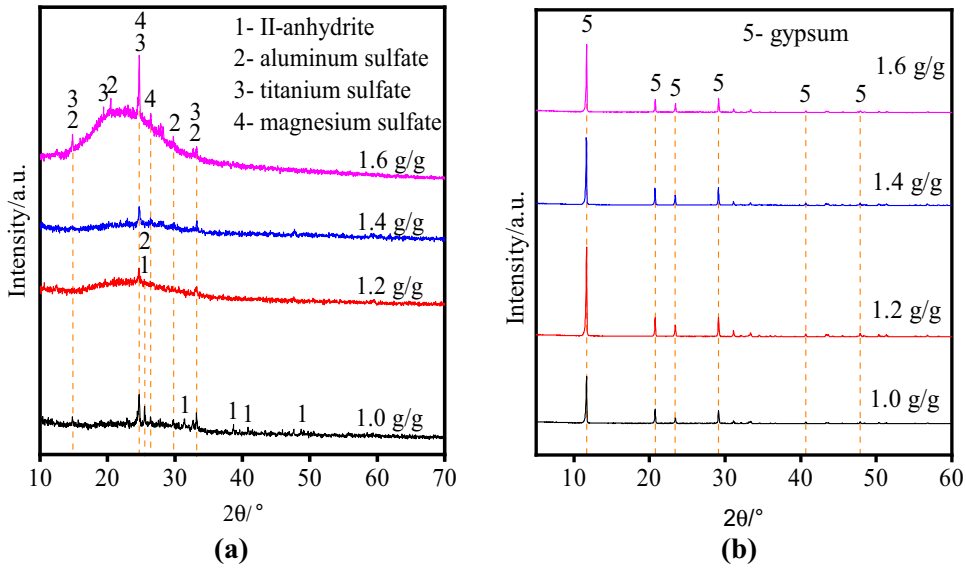

Fig. 4. XRD patterns of calcined slag (a) and leached slag (b) under different acid-slag ratios.

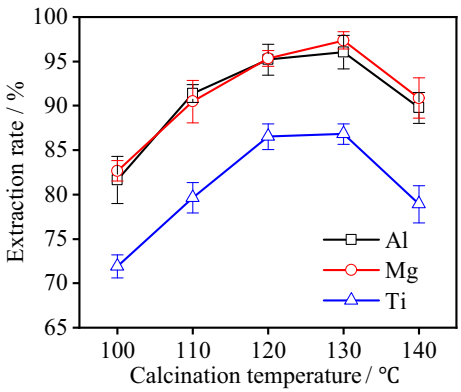

Fig. 5. Effect of calcination temperature on extraction rate of Ti, Mg, and Al components.

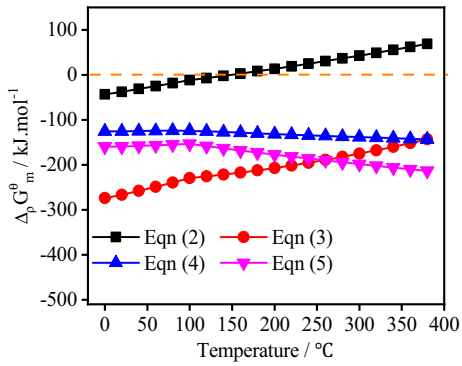

Fig. 6. Gibbs free energy of Ti, Mg, and Al fractions in TBFS reacting with sulfuric acid.

Gibbs free energy results for the chemical reaction in Eqs. 1, 2, 3, 4, and 5 are shown in Fig. 6, which shows that the Gibbs free energy of all reactions is < 0 in the temperature range < 160°C, so all reactions can easily occur. Gibbs free energy of Eq. 2 is the largest, followed by Eqs. 4 and 5, and the smallest is Eq. 3, so the reactions of Mg^{2+}, Al^{3+}, and Ti^{3+} with H_2SO_4 are more likely to occur compared to the reactions of Ti^{4+} with H_2SO_4. The extraction rates of Mg and Al were also higher than that of Ti (Fig. 5). SO_2 is generated in formula 2 at all temperatures set by the experiment in theory, while in practice, SO_2 can only be detected by Ph paper when the calcination temperature is > 130° C. Perhaps when the temperature is low, the amount of SO_2 generated is lower, and it can be absorbed by the H_2O generated to form sulfuric acid again. However, when the calcination temperature is > 130°C, the components react violently with sulfuric acid, and too much SO_2 is generated to be absorbed by H_2O. As such, SO_2 escapes from the calcination system, resulting in a reduced amount of sulfuric acid, thus reducing the extraction rate of Ti, Mg, and Al components. Based on the above analysis, 130°C was selected as the optimized calcination temperature. Compared with the existing research on sulfuric acid leaching TBFS, this process can achieve higher component extraction rates and less acid gas production. If properly controlled, SO_2 can be fully absorbed without escaping into the air and causing pollution, making it a relatively clean resource treatment process.

XRD analysis results of the calcined slag are shown in Fig. 7a. When the calcination temperature is low, the products in the calcined slag mainly exist in amorphous phase. With the increase of calcination temperature, the characteristic diffraction peaks of II-anhydrite, aluminum sulfate, titanium sulfate, and magnesium sulfate appear in the calcined slag, and their number and intensity

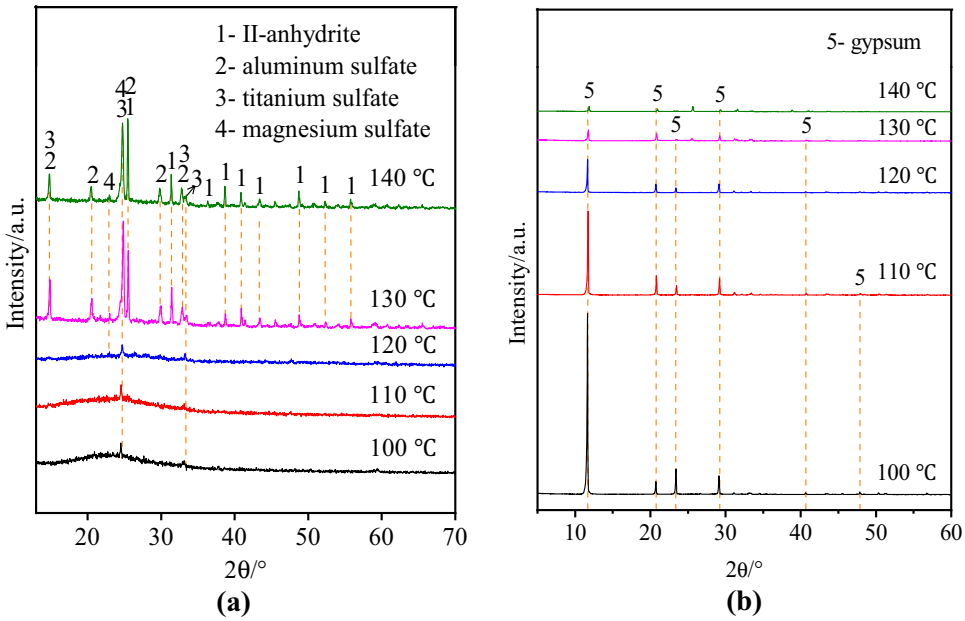

Fig. 7. XRD patterns of calcined slag (a) and leached slag (b) under different calcination temperatures.

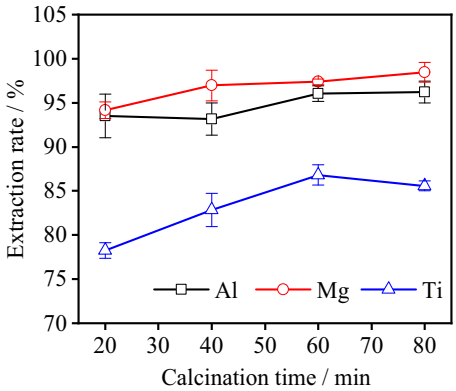

Fig. 8. Effect of calcination time on extraction rate of Ti, Mg, and Al components.

increase continuously, indicating that the increase of temperature is beneficial to the crystallization of each product phase. After water leaching, the main phase in the leached slag is gypsum (Fig. 7b). The peak type of its characteristic diffraction peak is relatively sharp, but the intensity decreases with the increase of calcination temperature. This occurs because highly crystalline II-anhydrite is less easily dissolved during leaching, so the time required to reach the supersaturation of gypsum is longer and the recrystallization time is shorter, resulting in the crystallized product having poor crystallinity.[14]

Effect of Calcination Time on the Extraction of Ti, Mg and Al from TBFS

Figure 8 shows the effect of calcination time on the extraction of Ti, Mg, and Al components. During the experiment, the acid-slag ratio was 1.4, and the calcination temperature was 130°C. The results show that the extraction rate of Ti increased with time and reached the highest value of 86.81% when the calcination time was 60 min; then, it tended to equilibrate. In the experimentally verified time range, the extraction rates of Mg and Al were all around 95%, which basically reached saturation, so the calcination time has little effect on the extraction rate of Mg and Al. Based on the energy saving, 40 min was selected as the optimized length of time for calcination, at which the extraction rate of Ti could reach 82.85%, Mg 93.16%, and Al 96.96%. The XRD pattern of calcined slag at different calcination times is show in Fig. 9a. With the increase of calcination time, the amorphous phase found in the calcined slag decreases, and the number and intensity of characteristic diffraction peaks of II-anhydrite, aluminum sulfate, titanium sulfate, and magnesium sulfate increase, indicating that the increase of calcination time is conducive to the crystallization of the products. As a result, the characteristic diffraction peak intensity of gypsum phase in water-leaching slag decreases with the increase of calcination time (Fig. 9b).

Micro Morphology of Slag Before and After Calcination

Figures 10a and 11a show the scanning electron microscope results of TBFS and calcined slag. Figure 10a shows that the morphology of TBFS particles is an irregular structure with angular and dense surfaces; the particle size is very uneven, and the particle surfaces are smooth. Figure 11a shows that there are many square slices of 2–4 μm side length in the calcined slag, which is the typical form of II-anhydrite.[15] The anhydrite square pieces are

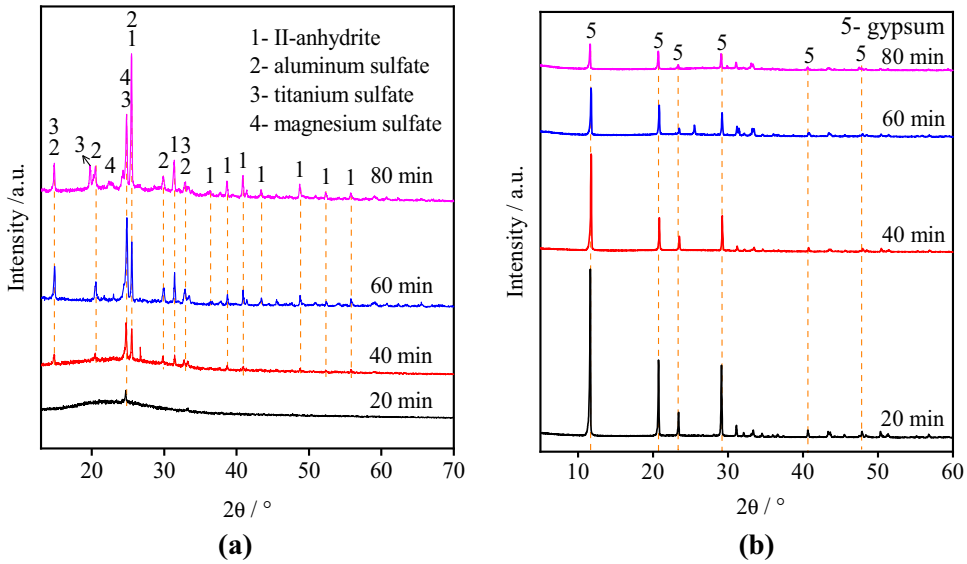

Fig. 9. XRD patterns of calcined slag (a) and leached slag (b) under different calcination times.

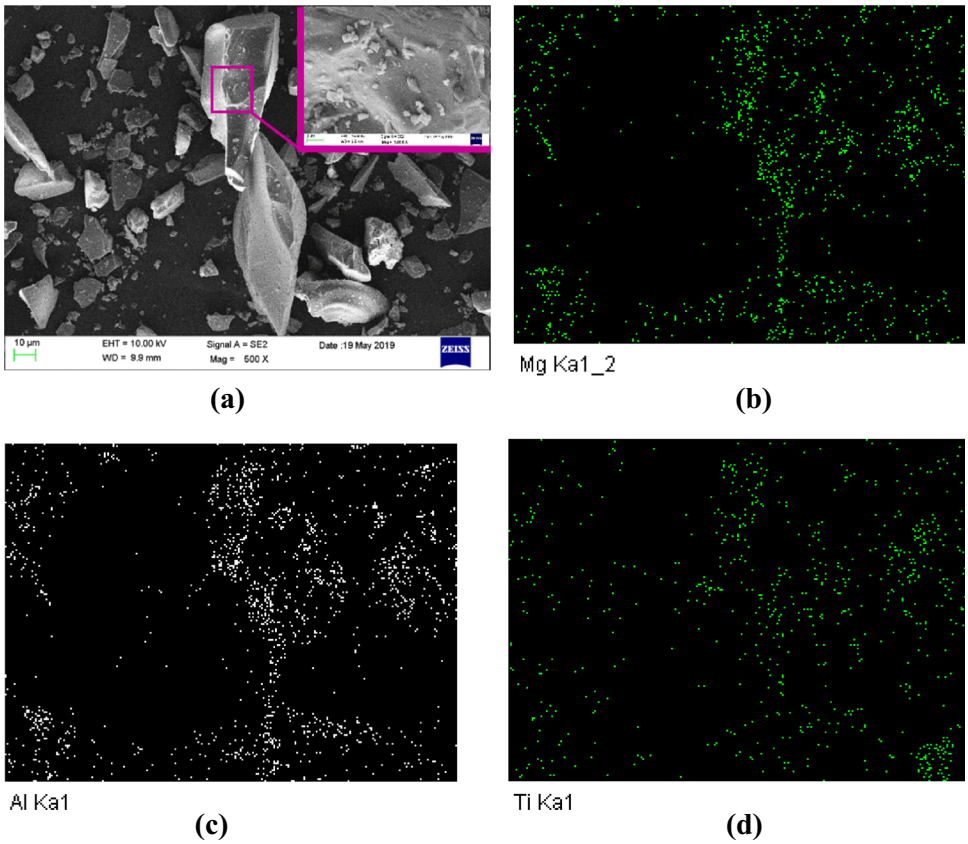

Fig. 10. The SEM–EDS picture of TBFS. (a) Full view. (b) Distribution of Mg^{2+}. (c) Distribution of Al^{2+}. (d) Distribution of Ti^{2+}.

overlapped in a disorderly manner and grow on the substrate without fixed morphology. The substrate may be composed of aluminum sulfate, magnesium sulfate, and titanium sulfate. The energy spectrum of the TBFS and A_1 area in calcined slag were analyzed for Ti, Mg, and Al elements. The results are shown in Figs. 10b, c, d and 11b, c, d; Ti, Mg, and Al elements are all present on the tested particles, and the distribution of the three metal elements is relatively uniform.

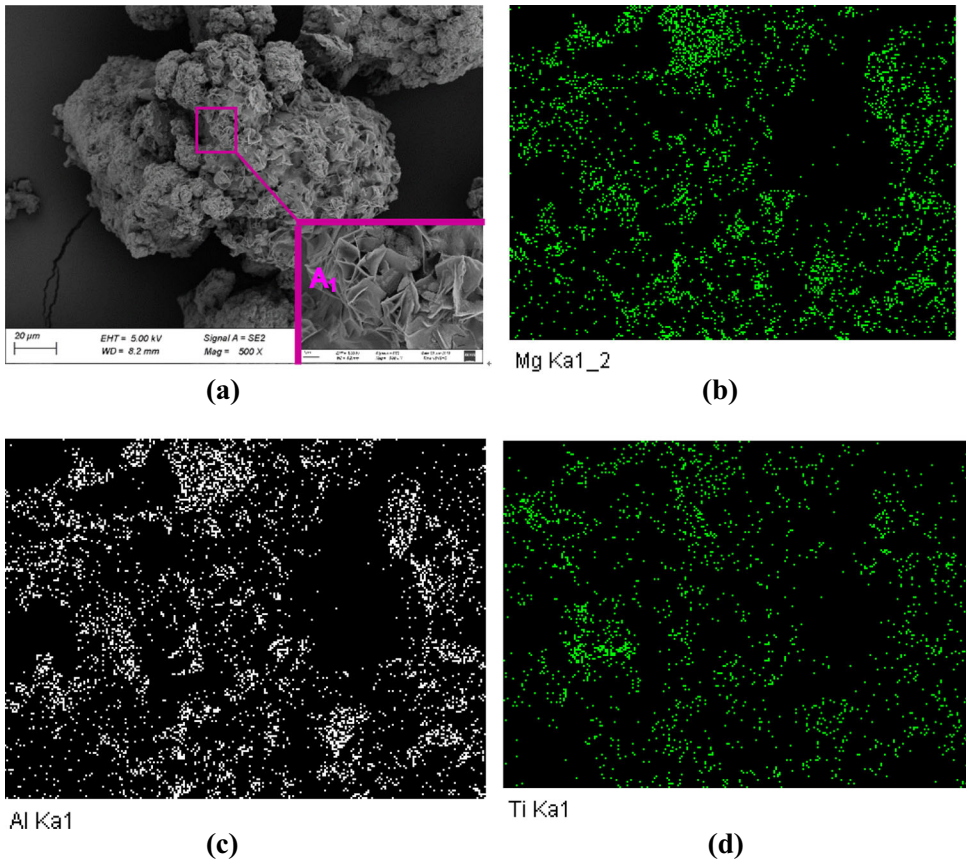

Fig. 11. The SEM–EDS picture of calcined slag. (a) Full view. (b) Distribution of Mg^{2+} of A_1. (c) Distribution of Al^{2+} of A_1. (d) Distribution of Ti^{2+} of A_1.

CONCLUSION

The chemical composition of TBFS includes CaO, SiO_2, TiO_2, Al_2O_3, and MgO as well as a certain amount of SO_3, Fe_2O_3, K_2O, MnO, Na_2O, and a small amount of F, BaO, SrO, and ZrO_2. The valence-variable elements Ti and Fe have two valence states each: Ti^{4+} and Ti^{3+} and Fe^{2+} and Fe^{3+}. The main mineral phase found was perovskite and some amorphous phase minerals. The microstructure of TBFS was found to be irregular, featuring edges and corners, dense surfaces, non-uniform particle sizes, and smooth particle surfaces. Ti, Al, and Mg components were extracted from TBFS with concentrated sulfuric acid by calcination. The main phases in the calcination slag were II-anhydrite, aluminum sulfate, titanium sulfate, and magnesium sulfate. The microstructure of the calcination slag showed that the II-anhydrite square pieces are overlapped in a disorderly manner and grow on the substrate without fixed morphology. No $CaSO_4{\cdot}2H_2O$ is formed in the calcination process, so the components' extraction rate is higher than that of traditional sulfuric acid leaching. The optimal conditions were found to be as follows: acid-slag ratio of 1.4, calcination temperature of 130°C, and calcination time of 40 min. The extraction rates of Ti, Al, and Mg were 82.85%, 93.16%, and 96.96%, respectively. In the calcination process, Ti^{3+} reacts with concentrated sulfuric acid to produce SO_2 gas, the amount of which is greatly affected by calcination temperature. When the temperature is low, the amount of SO_2 produced is decreased, and it can be absorbed by H_2O, one of the products, to form sulfuric acid again. When the temperature is high, more SO_2 is produced and cannot be absorbed by H_2O, so it is necessary to control the calcination temperature.

SUPPLEMENTARY INFORMATION

The online version contains supplementary material available at https://doi.org/10.1007/s11837-022-05557-w.

ACKNOWLEDGEMENTS

Financial support of this research was provided by Sichuan Science Provinces Science and Technology Support Program (2022NSFSC1072) and the research foundation of Mianyang Normal University (QD2021A06).

CONFLICT OF INTEREST

On behalf of all authors, the corresponding author states that there is no conflict of interest.

REFERENCES

1. Y. Kuwahara, T. Ohmichi, T. Kamegawa, K. Mori, and H. Yamashita, *J. Mater. Chem.* 20, 5052 (2010).
2. F. Valighazvini, F. Rashchi, and R. Khayyam Nekouei, *Ind. Eng. Chem. Res.* 52, 1723 (2013).
3. X. Liu and Z. Sui, *China Nonferrous Met.* 12, 1281 (2002).
4. Y. Xiong, C. Li, B. Liang, and J. Xie, *Chin. J. Nonferrous Met.* 18, 557 (2008).
5. Z. Huang, M. Wang, X. Du, and Z. Sui, *J. Mater. Sci. Technol. China* 19, 191 (2003).
6. H. Jiao, D. Tian, S. Wang, J. Zhu, and S. Jiao, *J. Electrochem. Soc.* 164, D511 (2017).
7. T. Jiang, H. Dong, Y. Guo, G. Li, and Y. Yang, *Miner. Process. Extr. Metall.* 119, 33 (2010).
8. J. Shi, Y. Qiu, B. Yu, X. Xie, J. Dong, C. Hou, J. Li, and C. Liu, *JOM* 74, 1 (2022).
9. W. Nie, S. Wen, Q. Feng, D. Liu, and Y. Zhou, *J. Market. Res.* 9, 1750 (2020).
10. A. Bahrami, M. Pech-Canul, C. Gutiérrez, and N. Soltani, *Appl. Surf. Sci.* 357, 1104 (2015).
11. M. Hadnadjev-Kostic, T. Vulic, R. Marinkovic-Neducin, D. Lončarević, J. Dostanić, S. Markov, and D. Jovanović, *J. Clean. Prod.* 164, 1 (2017).
12. M. Rashad, M. Mahmoud, I. Ibrahim, and E. Abdel-Aal, *J. Cryst. Growth* 267, 372 (2004).
13. H. Fan, X. Song, T. Liu, Y. Xu, and J. Yu, *J. Cryst. Growth* 495, 29 (2018).
14. A.N. Christensen, M. Olesen, Y. Cerenius, and T.R. Jensen, *Chem. Mater.* 20, 2124 (2008).
15. T. Sievert, A. Wolter, and N. Singh, *Cem. Concr. Res.* 35, 623 (2005).